Laser isotope separation of barium using an inhomogeneous magnetic field

W. A. van Wijngaarden and J. Li
Department of Physics, York University, Toronto, Ontario, Canada M3J 1P3
(Received 9 August 1993)

A barium atomic beam undergoes selective isotopic excitation by a dye laser to the $^1P_1$ state. This state radiatively decays back to the ground state or to the $(6s5d)D$ states, which are deflected out of the beam by an inhomogeneous magnetic field. The residual atomic beam is examined by a quadrupole mass spectrometer, and isotopic depletions of up to 60% are obtained using laser powers of a few hundred milliwatts. The isotopic splitting of the $^1S_0 \rightarrow {}^1P_1$ transitions for ^{136}Ba and the $F=\frac{5}{2}$ states of ^{135,137}Ba are measured relative to that for ^{138}Ba and agree well with those found previously.

PACS number(s): 28.60.+s, 31.30.Gs

I. INTRODUCTION

Lasers have been shown to be very useful for separating isotopes [1]. The significant advances in this subject are found in references in and to the excellent review article by Letokhov and Moore [2,3]. Laser isotope separation has significant advantages over the traditional gaseous diffusion and centrifuge methods. These methods depend on the relative mass difference of the isotopes and are therefore most efficient at separating the light isotopes. Huge multistage plants are needed to separate heavy isotopes. Lasers can selectively excite isotopes of even the heaviest elements due to their narrow linewidth. Hence the apparatus required for laser isotope separation is relatively simple, making the process more economical.

A commercial laser isotope separation method has been developed at Lawrence Livermore laboratory to separate U^{235} and U^{238} [4]. A three-step laser excitation is used to selectively ionize U^{235}. The ions are then collected using an electric field. The laser wave-lengths are resonant with transitions having large oscillator strengths to maximize the laser absorption. This, in turn, minimizes the overall cost.

Alternative isotope separation schemes that require only a single laser also exist. Bernhardt *et al.* [5–7] used radiation pressure to deflect an isotope out of an atomic beam of barium. A laser selectively excites one barium isotope from the $^1S_0$ ground state to the $^1P_1$ state. The atom acquires a momentum h/λ in the direction of the laser propagation each time it absorbs a photon. Here h is Planck's constant and λ is the wavelength. When the excited state spontaneously decays, the emitted photon does not have a preferred direction with respect to the laser beam. Hence the atom's momentum transverse to the atomic beam changes by Nh/λ after absorbing and emitting N photons. The deflection was limited by the metastable $(6s5d)D$ states to which the $^1P_1$ state could decay. The lifetime of the ^1D state is theoretically estimated to be about 0.5 sec [8,9]. Atoms trapped in this metastable state are not in resonance with the laser and hence their momentum no longer increases.

In this work, an inhomogeneous magnetic field is used to deflect barium atoms populating the metastable D states out of an atomic beam. This method of isotope separation, whereby a laser selectively excites an isotope, which is then deflected out of a beam using an electric or magnetic field gradient, has been proposed by several authors [1,10,11]. Naturally occurring barium has isotopes with atomic mass units 138 (71.7%), 137 (11.3%), 136 (7.8%), 135 (6.6%), 134 (2.4%), 132 (0.1%), and 130 (0.1%). The nuclear spin for the even isotopes is zero and for the odd isotopes is $\frac{3}{2}$. Separating barium isotopes is a strong test of an isotope separation method since the isotope shifts of the $^1S_0 \rightarrow {}^1P_1$ transition are smaller than those found in most other elements. In this paper, Sec. II briefly describes the method. This is followed by a description of the apparatus in Sec. III. Finally, data are presented and discussed in Secs. IV and V.

II. DISCUSSION OF METHOD

A schematic apparatus is shown in Fig. 1. An oven generates a collimated atomic beam containing a natural abundance of isotopes. The laser intersects the atomic beam orthogonally to eliminate the first-order Doppler

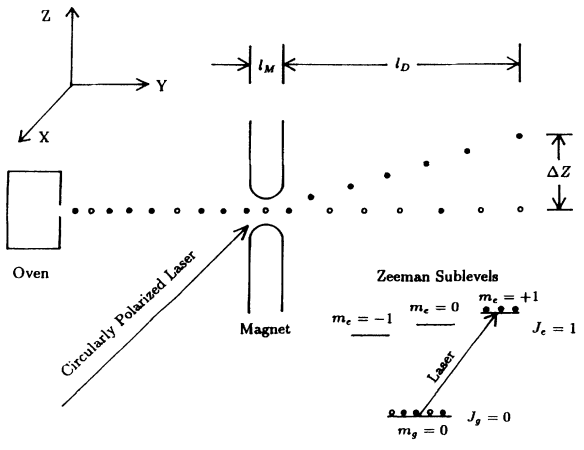

FIG. 1. Basic experimental arrangement. A laser selectively excites an isotope (filled circles) of an atomic beam. The excited atoms are subsequently deflected out of the beam by an inhomogeneous magnetic field.

shift which exceeds the isotope shift. Hence the laser can selectively excite a desired isotope out of the ground state as was done by Armstrong and Cooper in their study of photoionization of ^{138}Ba [12]. In the example shown in Fig. 1, atoms having a ground state of angular momentum $J_g=0$ and an excited state of angular momentum $J_e=1$ are considered. A circularly polarized laser pumps the atoms into the $m_e=1$ Zeeman sublevel of the excited state, which is then deflected using a Stern-Gerlach magnet to generate an inhomogeneous field. The acceleration of an atom in the direction transverse to the atomic beam continues as long as it occupies the excited state. The atom must be reexcited if it decays to the ground state during its passage through the magnet for it to continue to experience the deflecting force. The two resulting atomic beams have different isotopic compositions as illustrated in Fig. 1.

The acceleration of the excited atoms in the direction of the magnetic-field gradient is given by

$$a=g_J\mu_B\frac{dB}{dz}\Big/M\ , \tag{1}$$

where g_J is the Lande g factor, μ_B is the Bohr magneton, dB/dz is the magnetic-field gradient, and M is the isotopic mass. The deflection Δz measured at a distance l_D from the magnet is

$$\Delta z=\frac{al_Ml_D}{v^2}\ . \tag{2}$$

Here v is the thermal speed of the atoms and l_M is the magnet length which has been assumed to be much smaller than the distance to the detector. For the case of a thermal barium beam generated at 1000 K passing through a 5-cm-long magnet generating a field gradient of 10^4 G/cm and detected at a distance $l_D=100$ cm, the deflection is 0.1 cm. Hence the deflected atoms are spatially separated if the atomic beam divergence is less than 1 mrad.

The relevant barium energy levels are shown in Fig. 2. A laser excites the $^1S_0$ ground state to the $^1P_1$ state. This state radiatively decays either back to the ground state or

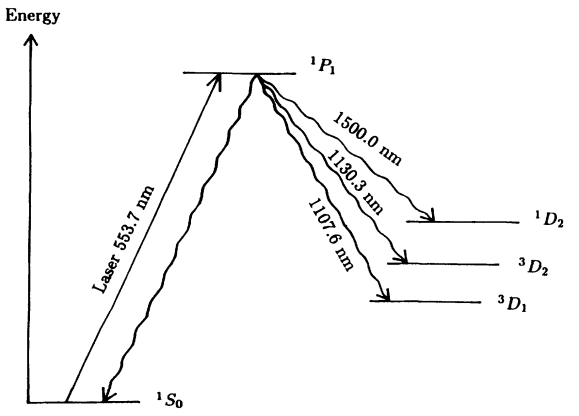

FIG. 2. Relevant barium energy levels. A laser excites the $^1S_0\rightarrow{}^1P_1$ transition. This state then radiatively decays (wavy lines) to the states shown.

TABLE I. Branching fractions from the $6s6p\ ^1P_1$ state. Data are taken from Ref. [13].

Lower level	Branching fractions
$6s6s\ ^1S_0$	0.9970±0.0003
$6s5d\ ^1D_2$	$(2.06\pm0.16)\times10^{-3}$
$6s5d\ ^3D_2$	$(9.0\pm1.4)\times10^{-4}$
$6s5d\ ^3D_1$	$(2.6\pm0.4)\times10^{-5}$

to the D states. The average number of laser photons needed to be absorbed by the atom in order to populate the metastable D states equals

$$\frac{1}{B(^1P_1\rightarrow{}^3D_1)+B(^1P_1\rightarrow{}^3D_2)+B(^1P_1\rightarrow{}^1D_2)}=334\pm30. \tag{3}$$

This expression was evaluated using the values for the branching ratios B that have been determined by Bizzarri and Huber and are listed in Table I [13]. Comparable values are given by two other groups [14,15]. The lifetime of the $^1P_1$ state has been measured to be 8.37±0.08 nsec [16]. Hence the minimum time required for an atom to absorb 334 photons is 2.8 μsec. This is less than the time it takes the atom to traverse either the laser beam (diameter ≈0.5 cm) or through the magnet.

The laser intensity required to saturate an atomic transition is given by

$$I_{\rm sat}=\frac{h\nu}{\sigma\tau}\ , \tag{4}$$

where σ is the absorption cross section, τ is the lifetime of the $^1P_1$ state, and $h\nu$ is the photon energy. For an electric dipole transition $\sigma\approx\lambda^2$, where λ is the transition wavelength. For the barium $^1S_0\rightarrow{}^1P_1$ transition, this yields a saturation intensity of 15 mW/cm^2. Such intensities are readily available from conventional dye lasers. Therefore, a high fraction of barium beam atoms can be populated in the D states as a result of the radiative decay of barium atoms laser excited to the $^1P_1$ state.

III. APPARATUS

A. Oven

The apparatus is shown in Fig. 3. An atomic beam is generated by heating the barium metal close to its melting point of 725 °C. A series of slits and baffles collimate the beam reducing its divergence angle to less than 1 mrad. The beam current was measured using a hot wire detector, not shown in Fig. 3 [17]. The neutral atoms were ionized upon striking a hot tungsten filament and the resultant ion current was measured by a sensitive ammeter (Keithley model 616). A stable ion current of about 1×10^{-10} A was achieved for hours at a time. Assuming the hot filament ionizes about 10% of the neutral atoms, we estimate the neutral beam current to be about 10^9 atoms/sec.

The oven is contained in a vacuum chamber that is pumped by a diffusion pump to a pressure of 3×10^{-7}

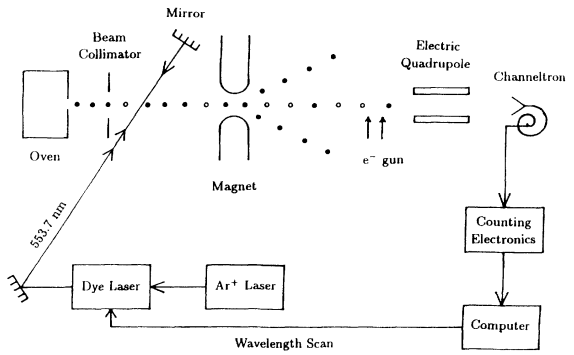

FIG. 3. Apparatus used for isotope separation.

Torr. It is separated from the rest of the vacuum system by a gate valve which could be closed to block the atomic beam facilitating the study of background signals. The hot wire current measured with the atomic beam blocked was 2×10^{-12} A. These background ions originate from either impurity atoms emerging from the tungsten filament or from the residual background gas.

B. Excitation of barium

The barium atoms are excited by a laser beam at a distance of 50 cm from the oven source. The laser light was generated by a ring dye laser (Coherent model 699) which was pumped by an Ar^+ laser. The ion laser power at 514 nm was 6 W. The dye laser produced 400 mW at 553.7 nm using Rhodamine 110 dye dissolved in ethylene glycol. The frequency of the ring laser is actively stabilized to give a manufacturer quoted linewidth at 0.5 MHz. The laser beam intersects the atomic beam orthogonally in order to eliminate the first-order Doppler shift. The residual transverse Doppler shift is estimated by multiplying the Doppler width by the 1 mrad beam divergence angle to be about 1 MHz. Light baffles prevent the excitation of the beam atoms by any laser light scattered from the vacuum chamber walls. Fluorescence resulting from the spontaneous emission of the excited atoms is viewed through a window facing the intersection of the laser and atomic beams. A fluorescent spot of approximately 1 mm in width was observed.

The laser excitation of the barium was studied using the apparatus shown in Fig. 4. Fluorescence was detected by a photomultiplier (Hamamatsu R928) whose linearity was checked using calibrated neutral density filters. The photomultiplier signal was sent to a lock-in amplifier (Stanford Research Systems 850) which was in turn interfaced to a computer. The reference signal was provided by a chopper that modulated the laser beam. The laser frequency was scanned across the $^1S_0\rightarrow{}^1P_1$ resonances of the various barium isotopes while the fluorescence data were taken. The laser frequency was monitored by measuring the laser power transmitted through a Fabry-Pérot étalon. The étalon consists of two mirrors supported by a zerodur spacer and is temperature stabilized to 0.03 °C. The manufacturer quoted free spectral range is 6.767 18 GHz.

Two plots of fluorescence intensity versus laser frequency are shown in Figs. 5 and 6. These data were tak-

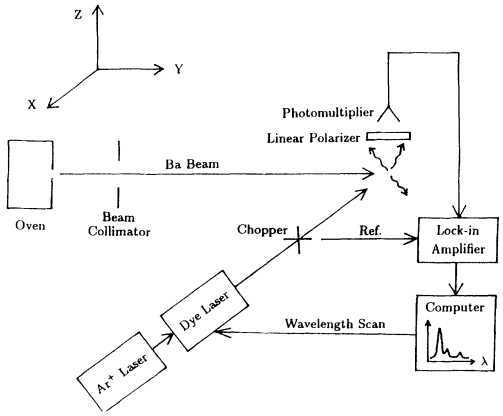

FIG. 4. Apparatus used to study laser excitation of barium.

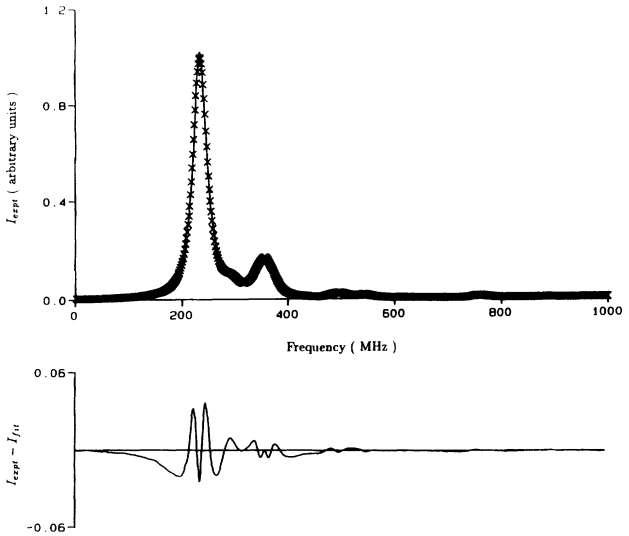

FIG. 5. Sample data of fluorescence polarized parallel to laser polarization. The data (crosses) I_{expt} were taken using a laser power of 1 mW and fitted to a curve I_{fit} (solid line) as is described in the text.

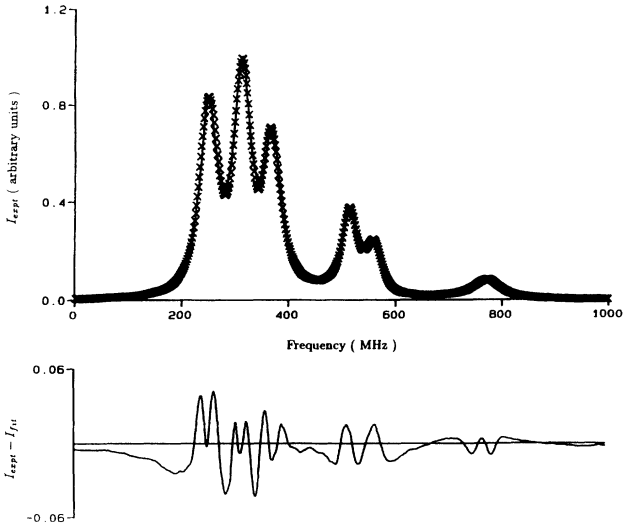

FIG. 6. Sample data of fluorescence polarized perpendicular to laser polarization. The data (crosses) I_{expt} were taken using a laser power of 1 mW and fitted to a curve I_{fit} (solid line) as is described in the text.

en using a dye laser power of 1 mW. In Fig. 5 fluorescence polarized parallel to that of the laser was detected. The spectrum is dominated by fluorescence produced by the even isotopes ^{138}Ba and ^{136}Ba which have zero nuclear spin. In Fig. 6 the detected fluorescence polarization is perpendicular to that of the laser. This spectrum clearly shows the effect of the hyperfine splitting for the ^{137}Ba and ^{135}Ba isotopes. The peak due to ^{138}Ba arises because the solid angle of detected light is not infinitely small.

The fluorescence spectrum was modeled as a sum of overlapping Lorentzian functions representing the various isotope and hyperfine peaks. The center frequencies of the Lorentzians were varied to obtain the best least-squares fit to the data. The difference between the fitted curves and the observed data are shown in Figs. 5 and 6. Note that the vertical scale has been magnified by a factor of 20.

The Lorentzian functions of the various isotopes in the modeled spectrum were assumed to have the same width. The full width at half maximum (FWHM) intensity giving the best least-squares fit to the data was 19.0±0.3 MHz. This is in excellent agreement with the natural linewidth 19.01±0.08 MHz computed using the measured lifetime $\tau=8.37\pm0.08$ nsec of the $^1P_1$ state [16]. The fluorescent lines broadened as the laser power increased. A best-fit linewidth of 31.4 MHz was observed when the laser power was 25 mW. At powers above 50 mW, the fluorescent intensity away from line center decreased less rapidly than predicted by a Lorentzian line shape as shown in Fig. 7. This distortion of the lineshape has been observed by other groups and has been attributed to optical pumping of the hyperfine levels of ^{135}Ba and ^{137}Ba [18]. Clearly, the isotopic selectivity of the laser excitation is highest at low laser power.

Table II lists the center frequencies found for the various isotopic and hyperfine transitions relative to the ^{138}Ba $^1S_0\rightarrow{}^1P_1$ transition. The 1.5% error bar results from uncertainty in calibrating the frequency axis using the Fabry-Pérot étalon. The frequency shift for the ^{136}Ba transition was found using the data shown in Fig. 5 while

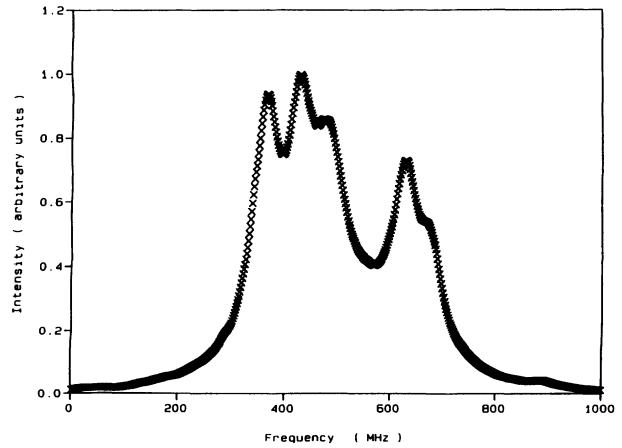

FIG. 7. Effect of power broadening. These data were taken as in Fig. 6 using a laser power of 50 mW. The data were not fitted since individual lines are distorted from a Lorentzian line shape.

TABLE II. Ba $^1S_0$-$^1P_1$ transition frequency relative to the transition on ^{138}Ba. The minus signs indicate that the ^{138}Ba transition is at a lower frequency.

		Δν (MHz)		
Isotope	F	Ref. [19]	Ref. [18]	This work
137	$\frac{5}{2}$	−62.8(6)	−63.0(6)	−63.3(9)
135	$\frac{5}{2}$	−121.6(6)	−120.1(7)	−120.0(18)
136	1	−128.9(5)	−127.5(13)	−128.6(19)
134	1	−143.0(5)	−142.8(12)	
137	$\frac{3}{2}$	−275.1(6)	−274.5(9)	−265.3(40)
135	$\frac{3}{2}$	−326.6(6)	−324.2(8)	−310.4(47)
135,137	$\frac{1}{2}$	−549.9(6)	−547.7(11)	−520.5(78)

the results for the other isotopes were obtained from the data shown in Fig. 6. A single value for the transition resulting from the $F=\frac{1}{2}$ ^{135}Ba and ^{137}Ba states is given since the two fluorescence lines were not resolved. Table II also lists results obtained previously. In Ref. [19], two atomic beams were used, one consisting of ^{138}Ba and the other of a different barium isotope. Two dye lasers excited the atoms. The frequency difference of the two lasers was determined by measuring their beat frequency. In Ref. [18], a single dye laser was scanned across the $^1S_0\rightarrow{}^1P_1$ resonance of a beam composed of natural barium. The frequency was monitored by passing the laser through a Fabry-Pérot interferometer having a free spectral range of 38.748(10) MHz. The fluorescence lines were fitted using a modified Lorentzian lineshape to obtain a satisfactory fit to the data. The line shapes were also power broadened having a FWHM of 29 MHz. The three experiments give results for the $F=\frac{5}{2}$ ^{137}Ba, ^{135}Ba, and ^{136}Ba frequency shifts that agree well with each other. However, our results are smaller for the $F=\frac{3}{2},\frac{1}{2}$ ^{137}Ba and ^{135}Ba frequency shifts. This indicates a possible systematic error such as would be caused by a nonlinearity in the frequency scan of our laser. This was checked by measuring the time needed to scan the laser frequency over successive free spectral ranges of the Fabry-Pérot étalon ($\nu_{FSR}=6.767\,18$ GHz). No scanning nonlinearity was evident. It would be useful to repeat this test using an étalon having a smaller free spectral range, but unfortunately none was available.

C. Isotope separation and detection

Atoms occupying the metastable D states are deflected out of the atomic beam by an inhomogeneous magnetic field as illustrated in Fig. 3. The magnetic field is generated by appropriately shaped magnetic pole pieces as is described by Ramsey [17]. The field gradient was estimated by deflecting sodium atoms in a Stern-Gerlach experiment to be 10^4 G/cm. The magnet produces a fringing field at the laser atomic beam interaction region, which is located 50 cm from the magnet. This field was measured by a Hall effect gaussmeter to be 12 G. It Zeeman splits the energy levels of the $^1P_1$ state. This in turn increases the number of peaks in the fluorescence spectrum complicating the isotopic selectivity of the laser ex-

citation. Two coils were therefore used to reduce the fringing field to less than 10 mG.

A quadrupole mass spectrometer (Balzers model QMG101A) analyzed the atomic beam propagating in the y direction. The spectrometer was located a distance of 50 cm from the magnet. It is contained in a vacuum chamber that was pumped to a pressure of 2×10^{-7} Torr by a diffusion pump. A liquid nitrogen trap removed condensable vapors such as pump oils which otherwise produced backgrounds in the barium mass range. The neutral beam atoms were ionized by an electron beam of about 10 μA. Electron energies of 100 eV were found to maximize the ion current. The barium ions then passed through the 20-cm-long quadrupole rods. The transmitted ions were detected by a channeltron held at a potential of -2600 V with respect to ground. The resulting electronic pulses were amplified (ORTEC 485 and ORTEC 9301), filtered by a discriminator (ORTEC 406A), and counted by a ratemeter (ORTEC 449). The ratemeter was interfaced to a computer which recorded the count rate as a function of the mass transmitted by the quadrupole spectrometer. In our experiments, the maximum count rate observed was 10^4 counts per second. The linearity of the electronics was checked using a pulse generator.

IV. RESULTS AND DISCUSSION

The results of a quadrupole mass scan of the barium atomic beam are shown in Fig. 8. The background measured with the beam blocked was a few hundred counts per second and was relatively constant over the mass range from 130 to 142 amu. Five barium isotopes $^{134-138}$Ba were detected. The peaks are asymmetric as predicted for quadrupole spectrometers [20]. The count rate decreases relatively slowly on the low mass side of a peak and falls steeply on the high mass side. The peaks have approximately the same width except for the anomalously narrow peak on the right side of ^{138}Ba. Side peaks such as this can be caused by the charging up of insulating material located on the quadrupole rods. This changes the ion trajectory and produces a narrow sidepeak located on the high mass side of a given peak [21]. The twenty-year-old spectrometer rods were examined but no obvious signs of contamination were visible. The above hypothesis was tested by loading the oven with cesium, which has only one stable isotope ^{133}Cs. The resultant mass spectrum had two peaks. The first peak was centered at a mass of 133 amu and had the same width as was found for the barium isotopes. The second peak was located near mass 134 amu and had a narrower width.

The quadrupole mass spectrum was modeled as follows. The line shape $F_i(m)$ of each isotope i was represented as the sum of two Lorentzian functions,

$$F_i(m)=\frac{1}{1+\left[\dfrac{m-m_i}{\Gamma_1}\right]^2}+\frac{s}{1+\left[\dfrac{m-m_i-\Delta m}{\Gamma_2}\right]^2}\,. \tag{5}$$

Here m_i is the isotope mass, s is a scaling factor less than unity, and Γ_1 and Γ_2 are the peak widths. The peak separation Δm was found to be slightly less than 1 amu. The complete mass spectrum $F(m)$ is found by summing over the isotopes,

$$F(m)=\sum_{i=134}^{138} a_i F_i(m)\,, \tag{6}$$

where a_i are the isotope abundances. The latter along with the other parameters are varied to obtain the optimum least-squares fit of $F(m)$ to the data. A typical fit to an observed mass spectrum is shown in Fig. 8. Similar values of a_i were obtained when Gaussian instead of Lorentzian functions were used in (5).

The effect of the laser on the mass spectrum was studied as follows. First, the quadrupole spectrometer was set to the mass of the isotope to be deflected. The laser frequency was tuned to minimize the count rate and a quadrupole mass scan was then taken. Figures 9 and 10 show data taken when the laser frequency was tuned to preferentially excite ^{138}Ba and ^{136}Ba, respectively. The

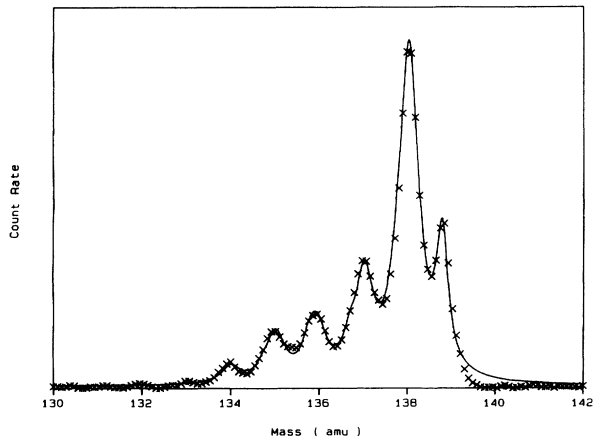

FIG. 8. Fit of modeled mass spectrum to data. The observed count rate is fitted to a curve as is described in the text. These data are taken with the laser off.

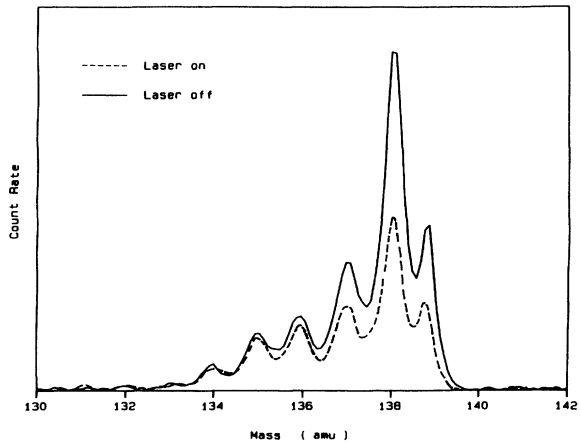

FIG. 9. Effect of laser on isotopic composition of atomic beam. The laser preferentially excited ^{138}Ba atoms which were deflected out of the atomic beam.

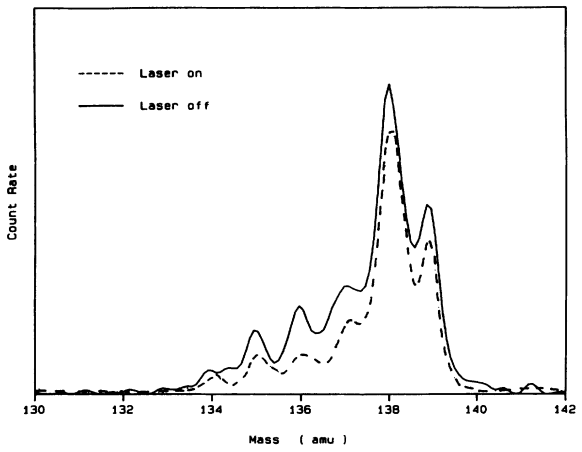

FIG. 10. Effect of laser on isotopic composition of atomic beam. The laser preferentially excited the $^{135-137}$Ba isotopes which were deflected out of the atomic beam.

laser was linearly polarized along the z direction and had a power of about 200 mW. Table III shows the effect of the laser on the isotope abundances, which were obtained by fitting the observed spectra. Smaller decreases in count rates were observed using less laser power. Other isotopes having overlapping resonances are also strongly affected. This is especially evident in Fig. 9 for ^{137}Ba which has a $^1S_0 \rightarrow {}^1P_1$ transition separated by 63 MHz from that of ^{138}Ba. Similarly in Fig. 10, the laser strongly decreases the peak count rate of ^{134}Ba.

The contribution of radiation pressure to the beam deflection was measured while the deflecting magnetic field was off. A 400-mW laser beam decreased the count rate measured at a mass of 138 amu by 35%. Lower laser powers as were used to obtain the data shown in Figs. 9 and 10 had a smaller effect. The count rate only decreased by 15% when the laser was retroreflected. This residual effect is likely caused by a difference in power of the two laser beams and their incomplete spatial overlap. Finally, the magnet was turned on and a 60% reduction in ^{138}Ba count rate was observed. The data shown in Figs. 9 and 10 were taken with the retroreflecting mirror present to minimize the effect of radiation pressure. Hence, a maximum of a quarter of the isotope depletions listed in Table III is due to radiation pressure.

The preceding analysis assumes the electron beam ionizes metastable and ground state atoms with equal probability. The ionization energy of the barium $^1S_0$ ground state is 5.212 eV [22], while that of the $(6s5d)D$ state is 2.96 eV. Data have been taken at electron energies up to 30 eV, showing that the ionization cross section of the D state is about twice that of the $^1S_0$ ground state [15,23]. Efforts are underway to take data at higher electron energies [24]. Unfortunately, expressions for ionization cross section such as obtained using the Born approximation are not sufficiently reliable to permit scaling to higher energies [25]. Hence, at an electron energy of 100 eV, the undeflected metastable atoms will be detected with greater efficiency than ground state atoms. Therefore the actual isotopic depletion is larger than that indicated in Figs. 9 and 10.

TABLE III. Effect of laser on isotope abundances.

	$[a_i$ (laser off) - a_i (laser on)$]/a_i$ (laser off)	
Isotope i	Laser on ^{138}Ba resonance	Laser on ^{136}Ba resonance
138	51%	13%
137	34	31
136	15	69
135	9	34
134	3	74

The magnet deflects atoms occupying the Zeeman sublevels of the D states having Zeeman quantum number $m \neq 0$. The sublevel populations are strongly affected by the laser polarization. For the even isotopes, circularly polarized laser light can only excite the $m = \pm 1$ sublevels of the $^1P_1$ state, while linearly polarized light excites only the $m = 0$ sublevel. If we consider the electric dipole decay of the $m = 1$ sublevel of the $^1P_1$ state to the $^1D_2$ level, then 90% of the atoms end up in sublevels having $m \neq 0$. For the electric dipole decay of the $m = 0$ sublevel of the $^1P_1$ state to the $^1D_2$ level, 60% of the atoms end up in the $m \neq 0$ sublevels. The final distribution of atoms among the Zeeman sublevels of the D state is complicated by the nonelectric dipole decay of the $^1P_1$ state to the $^3D_2$ and $^3D_1$ states. For the odd isotopes, the hyperfine interaction further complicates the optical pumping. In our experiments, circularly polarized laser light was generated using a quarter wave plate. No dramatic differences in the amount of isotope depletion were found using linear or circularly polarized light.

V. CONCLUSIONS

We have shown how a single laser can selectively populate an isotope into an excited state that is then deflected out of an atomic beam by an inhomogeneous magnetic field. This method is readily applicable to states having accessible metastable states as are found in the group-II elements. It can also enhance the isotopic deflection achieved using radiation pressure which can be limited by trapping of atoms in metastable states. No additional lasers are needed to excite atoms out of the metastable state [6]. Indeed, the deflection by the magnetic field exceeds that due to radiation pressure if the impulse given by the field during the excited state lifetime τ is greater than the photon momentum h/λ, i.e.,

$$g_J \mu_B \frac{dB}{dz} \tau > \frac{h}{\lambda} . \tag{7}$$

This criterion is satisfied for an optical transition at 5000 Å and a field gradient of 10^4 G/cm, if the lifetime exceeds 1 μsec.

Finally, the required apparatus is readily straightforward. Only a single commercially available laser and a Stern-Gerlach magnet are required. We therefore conclude that this method is useful for isotope separation and/or enrichment.

ACKNOWLEDGMENTS

We would like to acknowledge the Canadian Natural Science and Engineering Research Council for financial support. We also wish to thank M. van Leeuwen for preliminary technical assistance and R. Helbing for the use of the quadrupole mass spectrometer.

[1] R. N. Zare, Sci. Am. **236** (2), 86 (1977).
[2] V. S. Letokhov and C. B. Moore, Kvant. Elektron. (Moscow) **3**, 248 (1976) [Sov. J. Quantum Electron. **6** (2), 129 (1976)].
[3] V. S. Letokhov and C.B. Moore, Kvant. Electron. (Moscow) **3**, 485 (1976) [Sov. J. Quantum Electron. **6** (3), 259 (1976)].
[4] J. A. Paisner, Appl. Phys. B **46**, 253 (1988).
[5] A. F. Bernhardt, D. E. Duerre, J. R. Simpson, and L. L. Wood, Appl. Phys. Lett. **25**, 617 (1974).
[6] A. F. Bernhardt, D. E. Duerre, J. R. Simpson, and L. L. Wood, Opt. Commun. **16**, 169 (1976).
[7] A. F. Bernhardt, Appl. Phys. **9**, 19 (1976).
[8] C. W. Bauschlicher, S.R. Langhoff, R. J. Jaffe, and H. Partridge, J. Phys. B **17**, L427 (1984).
[9] P. McCavert and E. Trefftz, J. Phys. B **7**, 1270 (1974).
[10] G. V. Skrotskii and G. I. Solomakho, Zh. Tekh. Fiz. **50**, 861 (1980) [Sov. Phys. Tech. Phys. **25**, 517 (1980)].
[11] S. G. Potapov, At. Energ. **66**, 45 (1989).
[12] D. J. Armstrong and J. Cooper, Phys. Rev. A **47**, R2446 (1993).
[13] A. Bizzarri and M. C. E. Huber, Phys. Rev. A **42**, 5422 (1990).
[14] D. A. Lewis, J. Kumar, M. A. Finn, and G. W. Greenlees, Phys. Rev. A **35**, 131 (1987).
[15] S. Trajmar, J. C. Nickel, and T. Antoni, Phys. Rev. A **34**, 5154 (1986).
[16] F. M. Kelly and M.S. Mathur, Can. J. Phys. **55**, 83 (1977).
[17] R. Ramsey, *Molecular Beams* (Oxford University Press, New York, 1956).
[18] P. E. G. Baird, R. J. Brambldy, K. Burnett, D. N. Stacey, D. M. Warrington, and G. K.Woodgate, Proc. R. Soc. London Ser. A **365**, 567 (1979).
[19] G. Nowicki, K. Bekk, S. Goring, A.Hanser, H. Rebel, and G. Schatz, Phys. Rev. C **18**, 2369 (1978).
[20] P. H. Dawson, *Quadrupole Mass Spectrometry And Its Applications* (Elsevier, Amsterdam, 1976).
[21] M. Golding (private communication).
[22] C. E. Moore, *Analyses of Optical Spectra,* Natl. Stand. Ref. Data Ser., Natl. Bur. Stand. (U.S.), NBS-34 (U.S. GPO, Washington, DC, 1970).
[23] B. A. Bushaw, B. D. Cannon, G. K. Gerke, and T. J. Whitaker, Opt. Lett. **11**, 422 (1986).
[24] P. Zetner (private communication).
[25] N. F. Mott and H. S. W. Massey, The Theory of Atomic Collisions (Clarendon, New York, 1971).